CrossMark

ORIGINAL PAPER

Permian oolitic carbonates from the Baoshan Block in western Yunnan, China, and their paleoclimatic and paleogeographic significance

Hao Huang[1] · Xiaochi Jin[1] · Fei Li[2] · Yang Shen[3]

Abstract Marine carbonate ooids are environment-sensitive and hence valuable for paleoclimatic and paleogeographic reconstructions. This paper describes Permian ooids from the Baoshan Block in western Yunnan, China, in order to offer a new means to refine the uncertain paleogeographic details of this Gondwana-derived block. Four major types of ooids (micritic ooids, compound ooids, leached ooids and half-moon ooids) are documented from the Hewanjie Formation in the northern and the Shazipo Formation in the southern Baoshan Block. These ooids are dated via biostratigraphic analysis to be Wordian–early Wuchiapingian and signify an ameliorated shallow-marine temperature for the Guadalupian strata of the Baoshan Block. Results of this study, coupled with literature data, reveal diachronous debut of Permian ooids among the Gondwana-derived blocks: mostly Sakmarian in Central Taurides of Turkey, Central Iran, Central Pamir and Karakorum Block versus Wordian–Capitanian in Baoshan Block, Peninsular Thailand and South Qiangtang. In contrast, Asselian–Sakmarian strata of Baoshan Block as well as Peninsular Thailand and South Qiangtang are characterized by glaciomarine diamictites. These observations suggest that the Baoshan Block was probably situated at a considerably higher paleolatitude under distinct influence of Gondwana glaciation during the Asselian–Sakmarian than those blocks yielding Sakmarian ooids. Moreover, marine ooids are virtually absent nearby the equator within the Permian Tethys, similar to the modern situation. The Baoshan Block is accordingly interpreted to drift to warm-water southern mid-latitudes during the Wordian–Capitanian and remain to the south of Central Iran, Karakorum Block and South China, which were equatorially located in the Capitanian.

Keywords Ooid · Baoshan Block · Permian · Gondwana · Paleoclimate · Paleogeography

Introduction

The formation of marine carbonate ooids is sensitive to physicochemical conditions of sedimentary environments, and oolitic limestones in strata thus record information critical for exploring paleoclimate and paleogeography in geological past (e.g., Lees 1975; Peryt 1983; Sandberg 1983; Opdyke and Wilkinson 1990; Rankey and Reeder 2009; Flügel 2010; Li et al. 2015b). Permian ooids have been reported in recent years among the so-called Gondwana-derived blocks (e.g., Gaetani et al. 1995; Kobayashi and Altiner 2008; Leven and Gorgij 2011b; Huang et al. 2015a, b), which probably lay at northern Gondwana margin during the late Paleozoic and experienced dynamic rift-drift evolution in the process of Gondwana disassembly (e.g., Sengör 1979; Sengör et al. 1988; Shi and Archbold 1998; Wopfner and Jin 2009; Metcalfe 2013). Although the Gondwana provenance, detachment from peri-Gondwana and subsequent northward drift of these blocks have been generally acknowledged, many aspects of their paleogeographic history are still highly uncertain in the context of

✉ Hao Huang
geohaohuang@gmail.com

1 Institute of Geology, Chinese Academy of Geological Sciences, 26 Baiwanzhuang Road, Beijing 100037, China

2 State Key Laboratory of Oil and Gas Geology and Exploitation, Southwest Petroleum University, 8 Xindu Avenue, Chengdu 610500, China

3 School of Earth Sciences and Resources, China University of Geosciences (Beijing), 29 Xueyuan Road, Beijing 100083, China

🙂 Springer

Fig. 1 Location of the Baoshan Block in western Yunnan, China, showing sampling sites of Permian oolitic carbonates
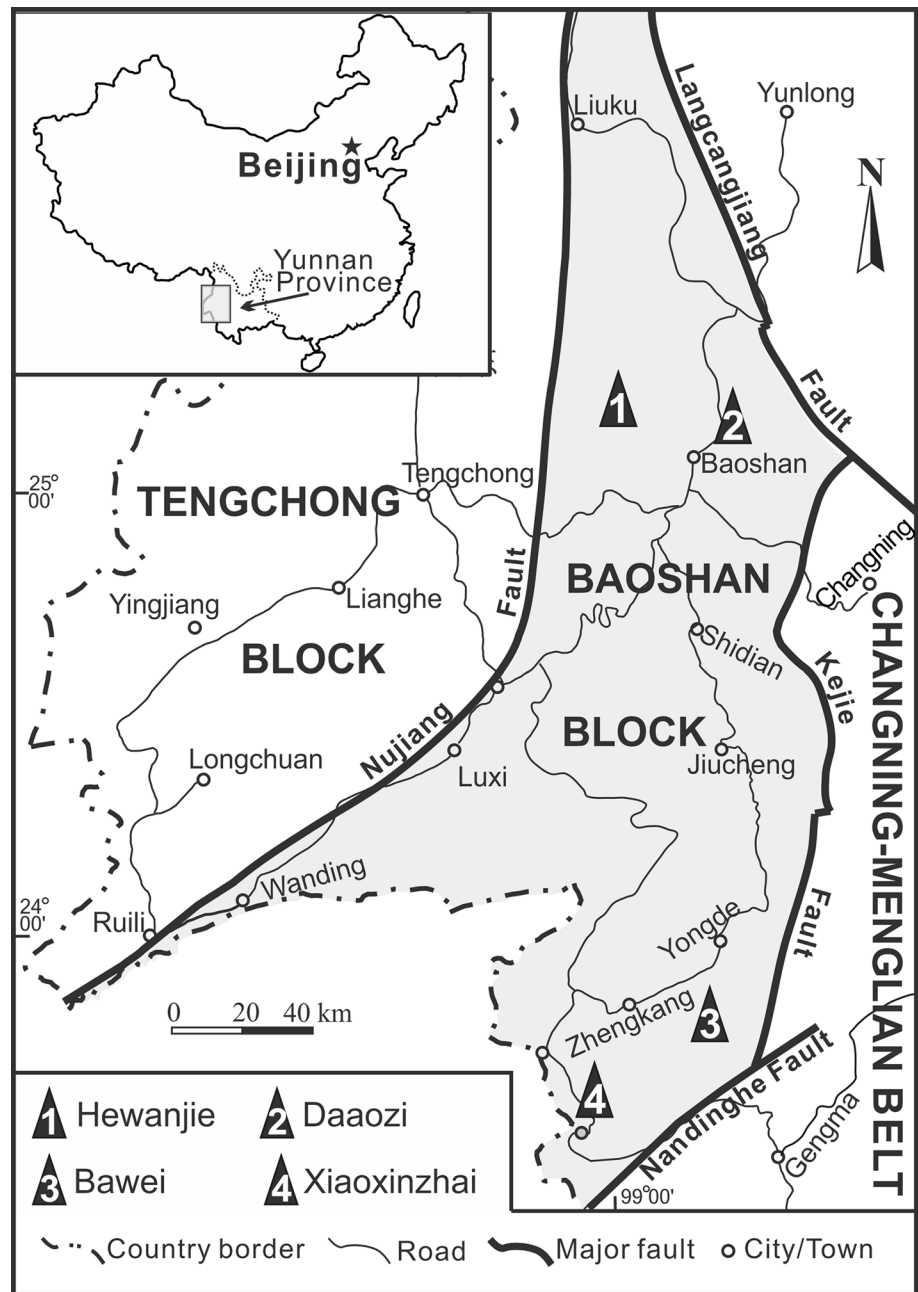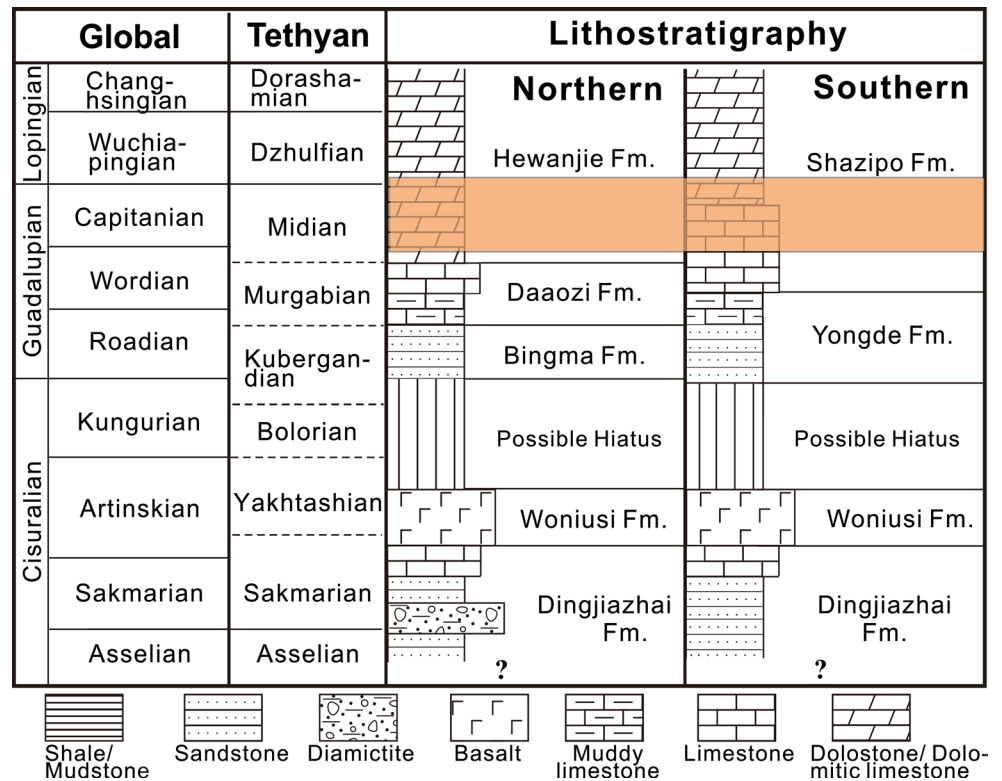

Permian Tethyan evolution (e.g., Liu et al. 2002; Scotese 2004; Ferrari et al. 2008; Metcalfe 2013). Even the overall configuration of their paleopositions relative to each other remains to be a subject of considerable controversy. The collective data on Permian ooids from these Gondwana-derived blocks might provide unique insights into this geological conundrum.

One of these Gondwana-derived blocks, the Baoshan Block in western Yunnan, China (Fig. 1), was firstly reported as containing Permian ooids in the 1980s (Lan et al. 1983; Sheng and He 1983; Geological Survey Team of Yunnan 1980; Bureau of Geology and Mineral

Resources of Yunnan Province 1990). Nevertheless, these ooids have been neither concretely figured nor studied in detail. Consequently, their paleoclimatic and paleogeographic significance remains hitherto insufficiently unraveled. Permian ooids in this area were still considered rare in a recent study focusing on the paleoclimatic meaning of the Permian carbonates in the Baoshan Block (Yan and Liang 2005). However, oolitic carbonates from Permian sections across the Baoshan Block have been discovered in our latest fieldworks and emphasize their potential importance. This paper elucidates the fabric, age and environmental implications of the Baoshan ooids and further compares the

Fig. 2 Composite stratigraphic columns of the Permian in the Baoshan Block. Shaded bar outlines the stratigraphic levels of oolitic carbonates. Global and Tethyan Permian chronostratigraphy based on Jin et al. (1997) and Leven and Gorgij (2011a), respectively

	Global	Tethyan	Lithostratigraphy	
			Northern	**Southern**
Lopingian	Chang-hsingian	Dorasha-mian	Hewanjie Fm.	Shazipo Fm.
Lopingian	Wuchia-pingian	Dzhulfian		
Guadalupian	Capitanian	Midian		
Guadalupian	Wordian	Murgabian	Daaozi Fm.	
Guadalupian	Roadian	Kubergan-dian	Bingma Fm.	Yongde Fm.
Cisuralian	Kungurian	Bolorian	Possible Hiatus	Possible Hiatus
Cisuralian	Artinskian	Yakhtashian	Woniusi Fm.	Woniusi Fm.
Cisuralian	Sakmarian	Sakmarian	Dingjiazhai Fm.	Dingjiazhai Fm.
Cisuralian	Asselian	Asselian	?	?

Shale/Mudstone · Sandstone · Diamictite · Basalt · Muddy limestone · Limestone · Dolostone/Dolomitic limestone

stratigraphic distribution of Permian ooids among several Gondwana-derived blocks. Our goal here is to utilize ooids as a sedimentological means to refine the details of the Permian paleoclimate and paleogeography of the Baoshan Block in relation to other Gondwana-derived blocks. Results of this study illustrate the valuable role that oolitic carbonates can play in constraining debatable paleogeographic and paleoclimatic reconstructions of terranes with dynamic geological history.

Geological background

The Baoshan Block in western Yunnan is bordered on the west by the Nujiang Fault and on the east by the Lancangjiang Fault, Kejie Fault and Nandinghe Fault (Fig. 1). The Permian of this block is composed primarily of siliciclastics in the lower part and carbonates in the upper part (Fig. 2). The lower Permian starts with the Dingjiazhai Formation, which mainly consists of shales, siltstones and fine sandstones at the base and a roughly tripartite succession of diamictites, pebbly mudstones and shales in the rest of this formation. This threefold succession has been regarded to be deposited in periods of glacial highstand, glacial retreat and deglaciation (Wang 1983; Jin 1994; Wopfner 1996; Jin et al. 2011) and may correspond to Glacial III with maximum ice sheets of the late Paleozoic Gondwana glaciation (Isbell et al. 2003, 2012). The pebbly mudstones and shales

are fossiliferous with brachiopods, bryozoans and crinoids. The top of the Dingjiazhai Formation contains carbonate beds of coquina facies rich in bryozoans, fusulinids and some conodonts, indicative a Sakmarian–Artinskian age (Fang et al. 2000; Wang et al. 2001; Ueno et al. 2002; Shi et al. 2011). Cool/temperate-water Gondwana affinity of these fossils is manifested by small solitary corals instead of massive reef-building elements, brachiopods with close faunal links to coeval Australian ones and rather impoverished fusulinids (Fang 1983, 1994; Fan and Fang 1992; Fang and Fan 1994; Shi et al. 1996; Wang et al. 2001; Shi et al. 2011). Based on these sedimentary and faunal features, the Baoshan Block has been reconstructed to be at the northern margin of Gondwana during the Cisuralian (Wang 1983; Jin 1994; Wopfner 1996; Metcalfe 2013).

The basalts of the Woniusi Formation, overlying the Dingjiazhai Formation, interrupted the normal marine sedimentation and probably represent the incipient intracratonic rifting of the Baoshan Block from the Gondwana (Wopfner 1996; Wopfner and Jin 2009). Limestone intercalations within these basalts yield fossils similar to those in the top of the Dingjiazhai Formation (Jin 1994). Paleomagnetic investigations of these basalts revealed a paleolatitude between 38°S and 42°S (Huang and Opdyke 1991; Ali et al. 2013; Xu et al. 2015). Hardgrounds occur at places on the top of the basalts, implying a possible sedimentary hiatus. Afterward, in the northern Baoshan Block, variegated fine siliciclastics of the Bingma Formation and overlying

thick carbonates reflect resumed sedimentation. The carbonate succession is subdivided into the Daaozi Formation of argillaceous limestones and limestones and the Hewanjie Formation of dolomitic limestones to dolostones. In the southern Baoshan Block, variegated siliciclastics and argillaceous limestones are grouped into the Yongde Formation, while the succeeding limestones and dolomitic limestones into the Shazipo Formation. Abundant brachiopods and corals as well as rare fusulinids of Wordian age occur in the argillaceous limestones of the Daaozi or Yongde Formation (Shi and Shen 2001; Wang et al. 2001; Jin and Zhan 2008). Upward, the limestones of the Shazipo Formation are rich in corals and fusulinids, while the dolomitic portion of the Shazipo or Hewanjie formations yields a foraminiferal *Shanita* fauna. These fusulinids and smaller foraminifera collectively denote a Wordian–early Wuchiapingian age (Sheng and He 1983; Wang et al. 2001; Jin and Yang 2004; Yang et al. 2004; Huang et al. 2005, 2009, 2015a, b). It needs to be clarified that although the Hewanjie Formation was dated previously to be Middle Triassic, recent studies have demonstrated that substantial parts of this formation are Guadalupian–Lopingian in age, based on foraminifera, conodonts and regional correlation (Jin et al. 2008). In contrast to the Cisuralian cool-water attributes, fossils and carbonates in the Guadalupian strata show progressive increase of warm-water features. For instance, fusulinid elements of Neoschwagerinids and Verbeekinids diagnostic for tropical/subtropical settings (Huang et al. 2009, 2015a, b) and massive *Wentzellophyllum* corals (Wang et al. 2001) are present in the Guadalupian strata. The Guadalupian carbonate facies belongs to the photozoan association characteristic for warm-water environment (Yan and Liang 2005). Judging from these pieces of information, climatic amelioration through the Cisuralian to Guadalupian is evident for the Baoshan Block and has been accounted by interplay of northward drift of this block toward paleoequator and concurrent global warming (Shi and Archbold 1998; Wopfner and Jin 2009).

Materials and methods

Ooid-bearing strata are developed in the Hewanjie Formation and Shazipo Formation in the northern and southern Baoshan Block, respectively. Samples of this study are from the Hewanjie Formation of the Daaozi Section and Hewanjie Section nearby Baoshan City and from the Shazipo Formation of the Bawei Section in Yongde County and the Xiaoxinzhai Section in Gengma County (Figs. 1, 2). Samples were collected at intervals of ca. 1 m in all sections except the Daaozi Section. From the Daaozi Section, collection was concentrated on the oolitic and fossiliferous beds. Thin sections of rock samples were prepared to observe ooid fabrics and analyze carbonate microfacies. Orientated thin sections for foraminiferal identification were made for biostratigraphic analysis. Classification of ooid types and procedures for microfacies analysis follow Richter (1983) and Flügel (2010), which use criteria, such as overall shape, cortical structure and diagenetic overprint, to classify ooids. Percentage of carbonate grains was estimated semiquantitatively by using the comparison chart of Baccelle and Bosellini (1965). Data in published literature were further compiled for comparing the stratigraphic distribution of Permian ooids between the Baoshan Block and other Gondwana-derived blocks.

Ooid features

Four dominant ooid types have been recognized in these strata: micritic ooids, compound ooids, leached ooids and half-moon ooids. The distinct fabrics and sedimentary features of each type are rendered as follows.

Micritic ooids

Micritic ooids with cryptocrystalline cortical lamination are the most common type in all examined sections (Fig. 3). They are more or less obscured regarding their cortical lamination, commonly lacking either tangential or radial pattern. The micritic ooids include mainly single normal or superficial ooids, as well as rare compound ooids. Their nuclei comprise fragments of ooids, bioclasts and peloids (Fig. 3g–i). The micritic ooids in the Daaozi Section were previously recognized as algal grains by Yang et al. (2004). However, regular and smooth concentric laminae (Fig. 3j) in these "algal grains" clearly distinguish them as ooids, rather than oncoids with algal origin. We interpret the micritization of these ooids to result from intense microboring of endolithic microorganisms (Bathurst 1966; Reid and Macintyre 2000). One line of evidence is the gradation from micritic ooids with distinct concentric lamination to almost structureless ooids with cortical banding completely obliterated. Besides, the micritic process appears to be centripetal replacement and commonly produces irregular boundary between the interior part and outer destructed part (Fig. 3k). The biogenic micritization is also witnessed by dark micritic rims of skeletal grains (Fig. 3d, f).

The micritic ooids are primarily distributed in two facies. The first facies is well-sorted oolitic grainstone with some peloids and poorly diversified foraminifera including *Shanita* and *Hemigordiopsis* (Fig. 3a–c). Oval ooids in this facies are 0.17–1.23 mm in diameter and densely packed (40–60 % rock). Foraminiferal tests are seldom fragmented, although usually indented by ooids. The second facies in which micritic ooids occur is moderately to
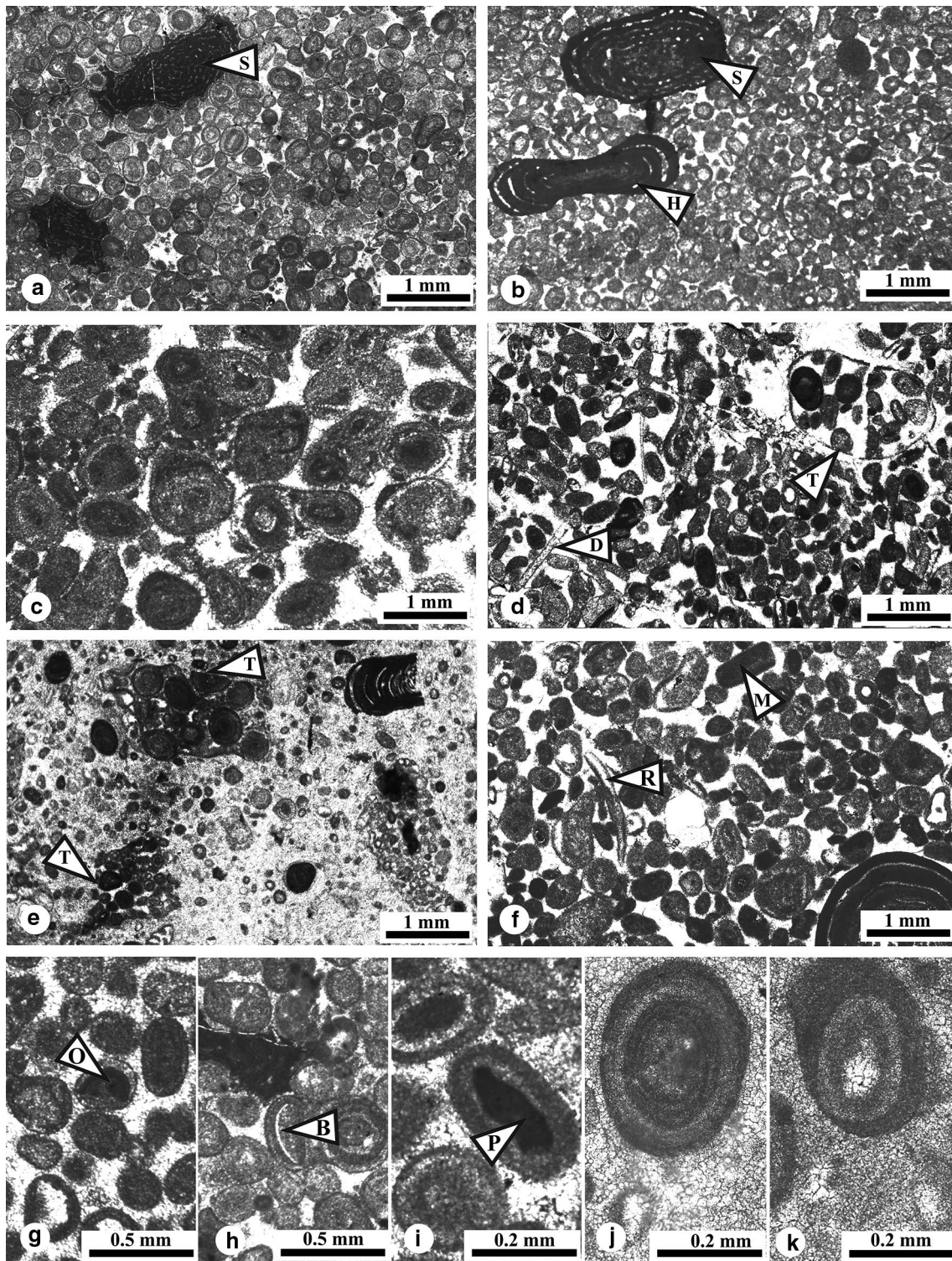
Fig. 3 Permian micritic ooids from the Daaozi Section, Hewanjie Section and Bawei Section in the Baoshan Block. **a–c** Well-sorted oolitic grainstone with foraminifera, *arrow S and H* point to foraminiferal specimens of *Shanita* and *Hemigordiopsis*; **d–f** moderately to poorly sorted skeletal and oolitic packstone to grainstone with lithoclasts, *arrow D* points to green algae (Dasyclads), *arrow T* to truncation of grains at the peripheries of lithoclasts, *arrow M* to micritic clasts and *arrow R* to micritic rim of one skeletal grain; **g–i** micritic ooids with broken ooid (*arrow O*), bioclast (*arrow B*) and peloid (*arrow P*) as nuclei, respectively; **j** one micritic normal ooid with conspicuously regular lamination in cortex; **k** micritic ooid with the central part dissolved and subsequently cemented by calcite spar, micritized outer part and irregular boundary between them

poorly sorted skeletal and oolitic grainstone to packstone and locally wackestone (Fig. 3d–f). Ooids in this facies are oval or elongated ellipsoidal and 0.19–0.56 mm in diameter. They make up 20–40 % of the rock, accompanied by peloids, aggregate grains, lithoclasts and bioclasts. Associated fossils are slightly more diverse and fragmented, comprising foraminifera, gastropods, green algae (Dasyclads) and phylloid algae. The lithoclasts are micritic or oolitic carbonates of variable size and subangular to round with conspicuous truncation at the boundaries (Fig. 3d–e). The concurrence of abundant ooids with low content of bioclasts of shallow-marine fossils, e.g., fusulinids and green algae adaptive to sunlit shallow sea, moderate to good sorting and grainstone to packstone texture of both facies, is diagnostic for oolitic shoals in recent and ancient carbonate record (e.g., Esteban and Pray 1983; Zeng et al. 1983; Tucker et al. 1990; Rankey and Reeder 2011; Flügel 2010; Pierre et al. 2010). In addition, the admixed micritic lithoclasts, locally micritic matrix and comparatively more diverse fossils likely hint a less winnowed and more interior platform setting for the second facies.

Compound ooids

Subspheroidal or lobate compound ooids (0.78–1.53 mm in diameter) are abundant in the Bawei Section and subordinate in the Daaozi Section (Fig. 4). Usually two or three single ooids are coated by concentric alternation of dark and light laminae into one compound ooid. The nuclei of these single ooids include skeletal grains and peloids and are dissolved to variable degree. Although the outermost coating includes up to ten laminae, its thickness is much less than the diameter of the interior core formed by the bounding of single ooids.

Interestingly, the compound ooids are confined in the lithoclasts which are well-sorted oolitic packstone and float in poorly sorted oolitic grainstone with peloids and bioclasts in the Bawei Section (Fig. 4a–d). These lithoclasts are considered to be generated in situ or nearby within the depositional basin, based on their variable size, poor rounding and the absence of peripheral truncation. These oolitic lithoclasts and accompanied ooids (0.21–0.79 mm in diameter) comprise up to 40–50 % of the rock (Fig. 4f–g). Some single ooids show asymmetrical growth with micritic laminae thickening in one direction (Fig. 4g), which possibly suggest non-turbulent periods for micritic enveloping to grow upward (Richter 1983; Strasser 1986; Flügel 2010). According to Flügel (2010), formation of compound ooids commonly undergoes two processes: (1) single ooids bound by encrustation or cementation in environment with restricted water circulation and reduced sedimentation rates and (2) regeneration of outer thin oolitic coating in agitated condition. Therefore, the coexistence of

asymmetrical single ooids and compound ooids, as well as micritic remains in the matrix, indicates alternation of low and strong water agitation.

Leached ooids

Many ooids have suffered diagenetic dissolution resulting in oomoulds, common in the Xiaoxinzhai, Bawei and Hewanjie sections (Fig. 5). The oomoulds are now occluded either by calcite spar or by euhedral rhomboidal dolomite. The leached ooids are commonly spherical to oval in shape and constitute 30–40 % of the rock. Many severely dissolved ooids only preserve rather thin outermost micritic rims (ca. 0.01 mm) or cortices with obliterated texture (Fig. 5a, h). Occasionally in less affected ooids, either skeletal (e.g., foraminifera and echinoids) or peloidal nuclei are coated by distinct concentric bandings (Fig. 5i).

Another significant feature is the distortion or rupture of these leached ooids. Some of them are distorted into flattened oval, duck-like or elephantine shape; several distorted ooids link together to form zig-zag chains (Fig. 5c, f, j, k). Such distortion has been regarded to result from weakening of ooids after dissolution of originally aragonitic portion (Richter 1983; Zeng et al. 1983; Wilkinson et al. 1984; Tewari and Tucker 2011; Li et al. 2015a). Some ooids have segmented outermost cortical layers around inner micritic cores (Fig. 5j). It is noticeable that the inner circumference of the ruptured outer layers is longer than the outer perimeter of inner cores. This particular phenomenon could be explained by the dissolution of in-between aragonitic layers and named "spalled cortices" by Wilkinson et al. (1984).

The leached ooids mainly occur in moderately to poorly sorted bioclastic and oolitic grainstone (Fig. 5b–c, e) and less commonly in well-sorted and densely packed oolite (40 % ooids) containing rare fossil skeletons (Fig. 5a, f). In the oolitic grainstone, ooids are 0.16–0.71 mm in diameter and make up 20–50 % of the rock, accompanied by aggregate grains, peloids, algae (Unganderella), foraminifera, echinoids and brachiopods. The fusulinid tests are often broken, indicating possible reworking or turbulence. Similar to the case of micritic ooids in the preceding section, these facies containing leached ooids are also interpreted to be formed in ooid shoals.

The other facies type in which the leached ooids are scattered is peloidal packstone (Fig. 5d). Cross-beddings are locally developed near the top of the stratigraphic beds of this facies type (Fig. 6). In the interstices between ooids in this facies, peloids are abundant and embedded in micritic matrix. The ooids are well sorted, but the bimodal size between white leached ooids (0.18–0.59 mm) and inter-ooid black peloids (mostly less than 0.12 mm) is conspicuous. The foraminiferal test and ellipsoidal peloids as ooid nuclei could reach 0.4 mm in diameter. If these ooids
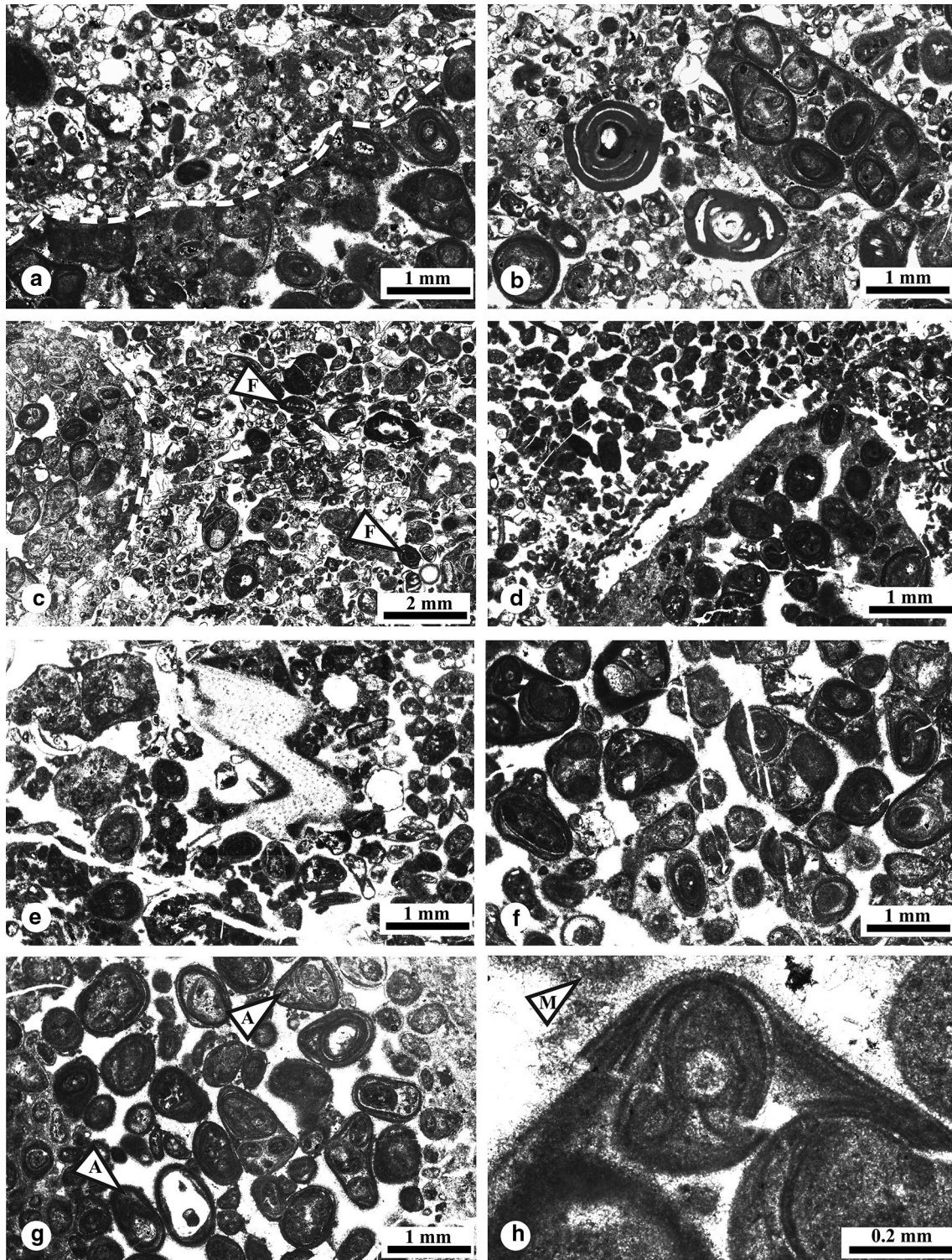
Fig. 4 Permian compound ooids from the Bawei Section in the southern Baoshan Block. **a** Sharp contact between a lithoclast (*below dashed line*) with compound ooids and host sediment with dissolved ooids (*above dashed line*); **b** poorly sorted bioclastic grainstone containing an oolitic lithoclast; **c** bioclastic grainstone with a rounded oolitic lithoclast (*left to the dashed line*) and smaller foraminifera (*arrow F*); **d** peloidal grainstone with a triangular oolitic lithoclast; **e** poorly sorted bioclastic grainstone with echinoid fragment; **f–g** close-up view of oolitic lithoclasts showing compound ooids and asymmetrical single ooids (*arrow A*); **h** high magnification of a compound ooid showing the thin outermost envelope and limited micrites (*arrow M*) in matrix
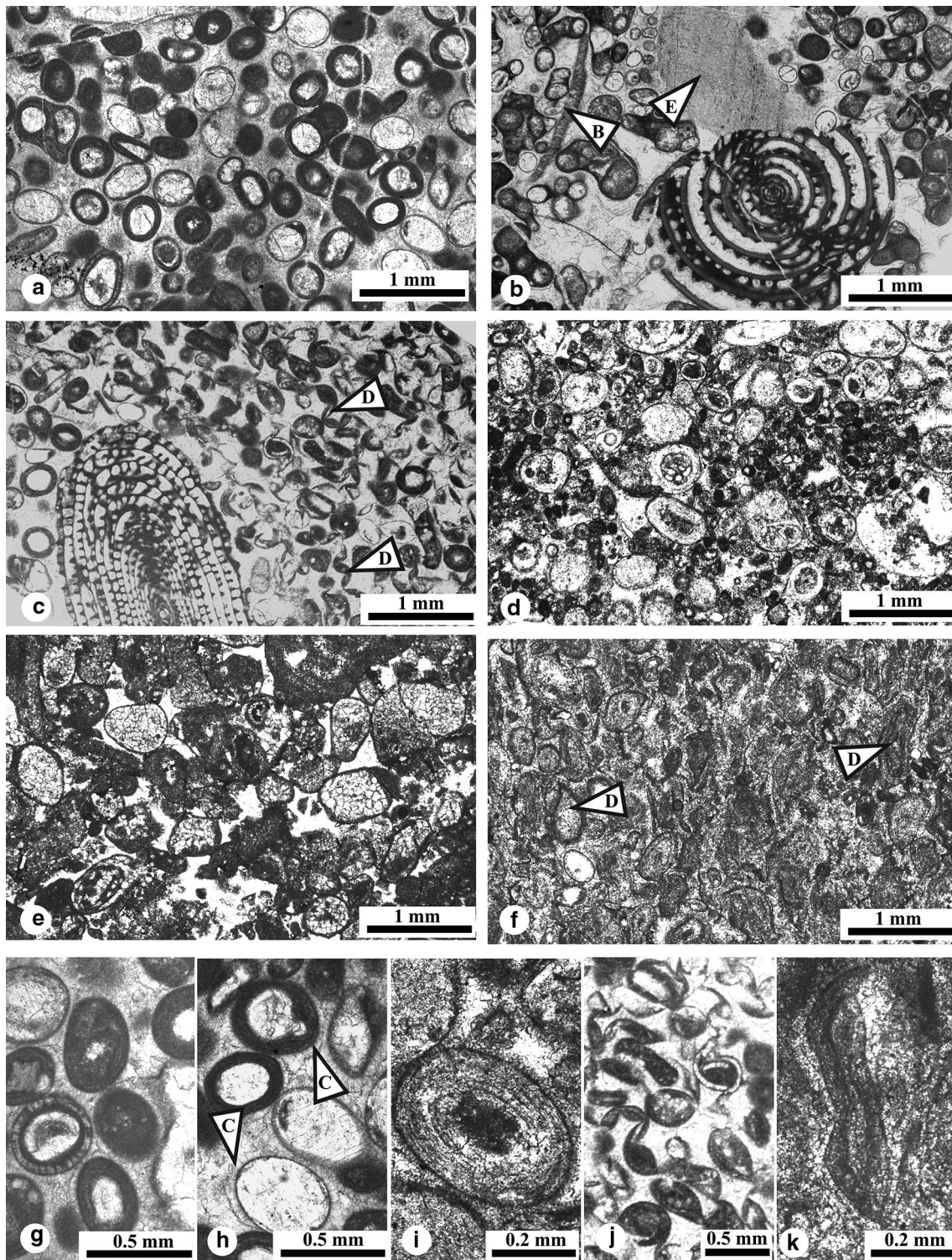
Fig. 5 Permian leached ooids from the Xiaoxinzhai Section, Bawei Section and Hewanjie Section in the Baoshan Block. **a**, **f** Well-sorted oolite with leached and distorted ooids, note the sample of f is strongly dolomitized; **b**, **c**, **e** moderately to poorly sorted bioclastic and oolitic grainstone, note leached ooids are occluded by rhomboidal dolomite in (**e**) and fusulinid *Armenina* and *Pseudodoliolina* in (**b**) and (**c**), respectively; **d** leached ooids floating among peloids in peloidal packstone; **g** selectively leached ooids against relatively well-preserved ooid with radial cortex; **h** close-up view of leached ooids showing early isopachous cementation; **i** less leached ooids with distinct concentric cortical lamination; **j**, **k** magnification of distorted ooids; *arrows B, C, D, E* refer to, respectively, brachiopods, early cements, distorted ooids and echinoids

Fig. 6 Cross-beddings of the oolitic packstone in the Bawei Section in the southern Baoshan Block

were produced in situ, it would be hardly conceivable that many peloids, which are smaller than the ooid nuclei, are not incorporated as the cores for further ooid growth. The agitation required for ooid production appears to be incompatible with relatively low water energy suggested by large quantity of peloids and the micrites in matrix. We, therefore, interpret these ooids and peloidal packstone

to be deposited nearby to each other and later intermixed together.

Half-moon ooids

The half-moon ooids exhibit a peculiar dichotomy between upper coarse sparitic and lower dense micritic halves (Fig. 7). The dual subdivisions of these ooids form excellent geopetal structure. The shape of these ooids is usually flattened oval or even deformed into curvy forms (Fig. 7b). Diameters fall between 0.2 and 0.73 mm when measured along their long axes. The bottom dark halves appear to result from the collapse of micritic ooids, as demonstrated, in rare instances, by plastic deformed but still differentiated nuclei and cortices in the lower portion (Fig. 7a, d). Isopachous cementation seems to prevent the complete collapse of the ooids (Fig. 7c, e). The upper void is commonly occluded by coarse blocky calcite.

These half-moon ooids with good sorting compose 60 % of oolitic packstone and are confined in one stratigraphic level of the Bawei Section. Associated allochems include some peloids and rare foraminifera. The matrix is micritic, but now partially dolomitized. Oolitic packstone can be found in the bank interior on the flanks of ooid shoals in
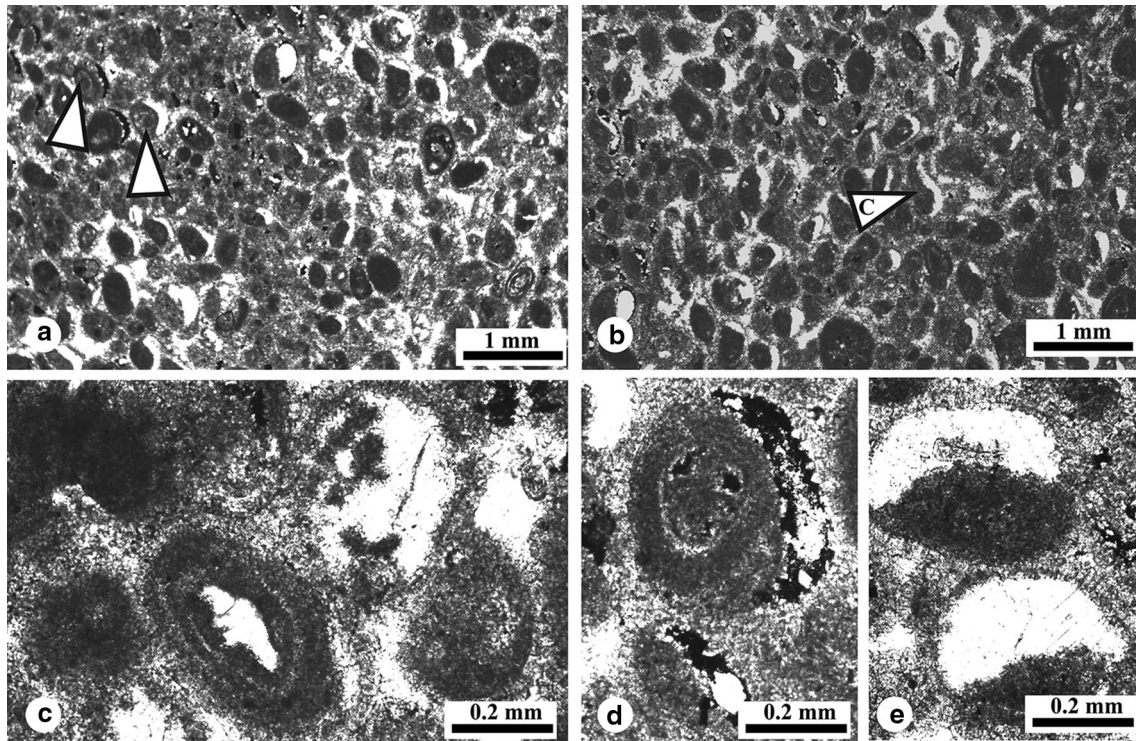

Fig. 7 Permian half-moon ooids from the Bawei Section in the Baoshan Block. **a**, **b** abundant half-moon ooids in well-sorted oolitic packstone, note the slightly compacted oval shape, or even curvy form (*arrow C*) and vague division of nuclei and cortices in micritic halves (*blank arrow*); **c** co-occurrence of ooids with concentric banding and ooids that are almost entirely leached; **d** close-up view of a half-moon ooid showing deformation of micritic portion; **e** sharp distinction of sparitic and micritic portions of a half-moon ooid, note the coarse blocky calcite cement in the upper part with relic micrite
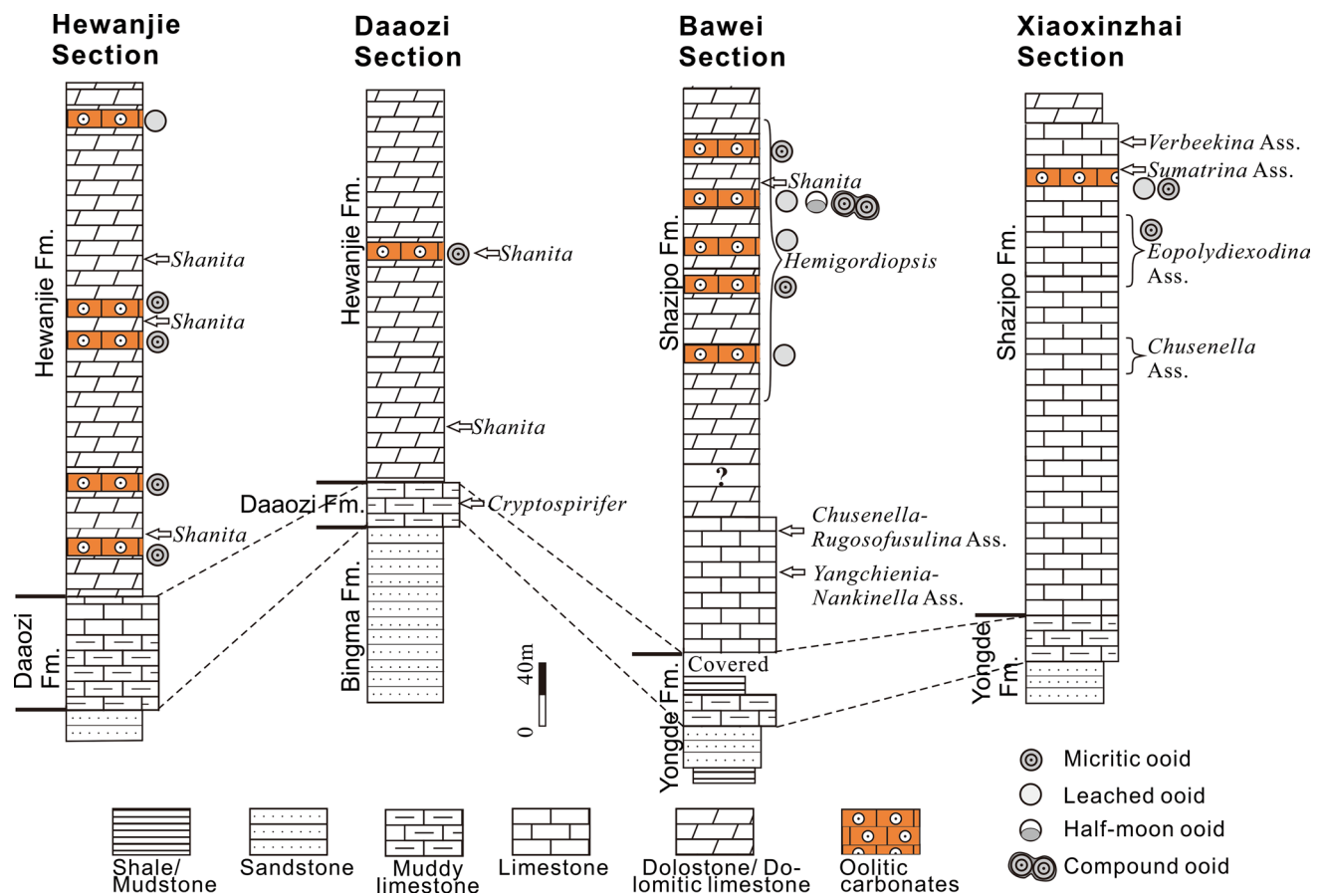
Fig. 8 Stratigraphic distribution of Permian ooids across the Baoshan Block. The Daaozi Section is modified based on our field observation from Yang et al. (2004), and the others are our measured sections

modern Bahamas (Harris 1983) and similar environments in geological record, e.g., Permian Grayburg Formation, Midland Basin of USA (Barnaby and Ward 2007).

Age constraints

The age of ooids in both the Hewanjie and Shazipo formations can be well constrained by foraminiferal biostratigraphy (Fig. 8). Within or between these oolitic beds occurs the *Shanita-Hemigordiopsis* foraminiferal assemblage in all sections except the Xiaoxinzhai Section. This assemblage is diagnostic for the northern peri-Gondwana and used to be considered to range from late Murgabian to possibly Wuchiapingian, based on non-fusulinid foraminifera and regional stratigraphic correlation (Brönnimann et al. 1978; Pronina 1988; Dawson et al. 1993; Leven 1997; Jin and Yang 2004; Huang et al. 2005). Its appearance as early as the Wordian, however, has been recently confirmed in Shan State of Myanmar, as it is associated or interbedded with Wordian fusulinids, e.g., *Neoschwagerina craticulifera* and *N. margaritae* (Win et al. 2011).

In the northern Baoshan Block, the Daaozi Formation in the Daaozi Section and nearby areas contains brachiopod *Cryptospirifer* fauna, coral *Wentzellophyllum* fauna and sporadic fusulinids. These fossils collectively attest to a Wordian age, at least not younger than the Capitanian (Shi and Shen 2001; Wang et al. 2001; Jin and Zhan 2008; Jin et al. 2011). The oolitic beds in the overlying Hewanjie Formation are tens to even hundreds of meters above the Daaozi Formation and thus should not be older than the Wordian age. This interpretation is congruent with the temporal data from foraminifera discussed above. These lines of evidence altogether assign a Capitanian–early Wuchiapingian age to the oolitic carbonates in the northern Baoshan Block.

Precise age information is furnished by fusulinid biostratigraphy for the Permian ooids in the southern Baoshan Block. Fusulinid *Yangchienia–Nankinella* assemblage and *Chusenella–Rugosofusulina* assemblage occur more than 100 m below the lowest occurrence of the oolitic beds in the Bawei Section. The age of these two assemblages is Murgabian–Midian in Tethyan Permian scale, approximating Guadalupian in global standard (Huang

et al. 2015b, 2016). Besides, all the oolitic beds are located within the stratigraphic range of the *Hemigordiopsis* in this section, and some *Shanita* specimens occur between the top oolitic beds. Based on these data, the oolitic beds in the Bawei Section are designated an age of Capitanian to possibly Wuchiapingian. In the Xiaoxinzhai Section, sporadic carbonate ooids occur as low as the top of the *Eopolydiexodina* assemblage, whereas abundant ooids are associated with fusulinids belonging to the *Sumatrina* assemblage. Biostratigraphic analysis determines the *Eopolydiexodina* assemblage to be Murgabian (approximately late Roadian–Wordian) and the *Sumatrina* assemblage to be Midian (approximately Capitanian) in age, respectively (Huang et al. 2009, 2015b). Accordingly, sporadic ooids in this section firstly appear in the Wordian strata, while oolitic carbonates become common in the Guadalupian strata.

Paleoclimatic and paleogeographic implications

Both laboratory and field researches have demonstrated that the formation of marine carbonate ooids requires the convergence of multiple physiochemical factors, majorly including clean, shallow and warm seawater supersaturated with carbonate, presence of nuclei and bottom agitation, although the details of ooid genesis remain incompletely understood (Newell et al. 1960; Bathurst 1975; Davies et al. 1978; Deelman 1978; Simone 1980; Richter 1983, Tucker et al. 1990; Flügel 2010; Hearty et al. 2010; Reeder and Rankey 2008; Rankey and Reeder 2009). At the global scale, marine carbonate ooids are largely confined within 40°N and S in both modern and Phanerozoic oceans (Lees 1975; Opdyke and Wilkinson 1990; Li et al. 2015b). Opdyke and Wilkinson (1990) further argued that Holocene aragonitic ooids mostly form where summer temperatures of sea-surface water exceed ca. 25 °C. Therefore, warm seawater is a precondition for marine ooid production and oolitic feature can be regarded as diagnostic for Phanerozoic warm-water carbonate facies (Lees and Buller 1972; Lees 1975; Nelson 1988; James 1997; Flügel 2010). The abundant Permian ooids recovered from the Baoshan Block thus represent a warm and shallow-marine environment for carbonate sedimentation. Moreover, these ooids are associated with peloids, aggregate grains, green algae and fusulinids (Figs. 3, 4, 5). These grains constitute a typical Photozoan association of carbonate facies, also reflecting shallow and warm sedimentary realm (James 1997; Flügel 2010).

The signature of warm-water condition from the studied ooids strengthens previous arguments that the paleoclimate of the Baoshan Block significantly ameliorated from the Artinskian onward, based on sedimentological and fossil evidence. The Asselian–Sakmarian cool-water condition has been suggested by diamictites of probable glaciomarine

genesis in the lower part of the Permian in the Baoshan Block (Wang 1983; Jin 1994; Wopfner and Jin 2009). A marked shift from siliciclastic environment to carbonate setting took place at the beginning of the Artinskian (Jin et al. 2011). Furthermore, Yan and Liang (2005) recognized that the Artinskian carbonate grains are dominantly bryozoans and crinoids with no non-skeletal grains, whereas the Guadalupian grains are more diverse with warm-water elements, e.g., fusulinids, green algae and peloids. However, they posited that Permian ooids were rare, due to the absence of ooids in their Permian collections. They further assigned the Artinskian grain association to bryonoderm-extended type indicating warm-temperate condition and the Guadalupian association to chloroform type of tropical/subtropical warm condition (following the classifications of Nelson 1988 and James 1997). On the other hand, brachiopods, corals and fusulinids consistently changed from low diversified fauna of cool- or at least temperate-water Gondwana affinity in the Cisuralian to more diverse composition with progressive influx of warm-water taxa in the Guadalupian (Shi and Archbold 1998; Wang et al. 2001; Huang et al. 2015a, b).

Besides the Baoshan Block, Permian oolitic limestones have been documented from several other Gondwana-derived blocks (Fig. 9). Permian ooids have been recognized from both lower and upper Permian of the Aladağ Unit in Central Taurides, Turkey. Oolitic grainstone facies occurs between Sakmarian *Paraschwagerinia pseudomira* and *Robustoschwagerina nucleolata* fusulinid zones at the Hadim area (Kobayashi and Altiner 2008, pl. 1, Fig. 2), and ooids associated with late Asselian–early Sakmarian fusulinids occur at the base of the Eskibey Section (Okuyucu 2008). A 40- to 60-cm-thick oolitic bed also occurs in the uppermost Permian in the Hadim region (Ünal et al. 2003, pl. 3, Figs. 4–8), and its Dorashamian age is controlled by the underlying foraminiferal *Paradagmartia* zone and overlying early Triassic stromatolitic boundstone. The Aladağ Unit has been considered an internal part of Taurus domain which shows typical Gondwana affinity based on the features of its basement, Paleozoic–Mesozoic cover and tectonic evolution (Göncüoğlu et al. 2007; Moix et al. 2008).

Oolitic limestones also characterize the base of the Early Permian Chili Formation at Halvan mountains in the Kalmard area, Central Iran (Leven and Gorgij 2011b, Fig. 2 and pl. V, Fig. 1; Shahraki et al. 2015, Fig. 5e). The Chili Formation postdates a Bashkirian–Asselian hiatus and underlies carbonates with conodonts indicative Tastubian substage (early Sakmarian) and Kalaktash fusulinid assemblage of Sakmarian age. The ooids at the base of this formation are then well constrained to be early Sakmarian in age. The Central Iran and North Iran (Alborz mountains) are collectively interpreted to be an extension of Arabian platform at northern peri-Gondwana during the most time
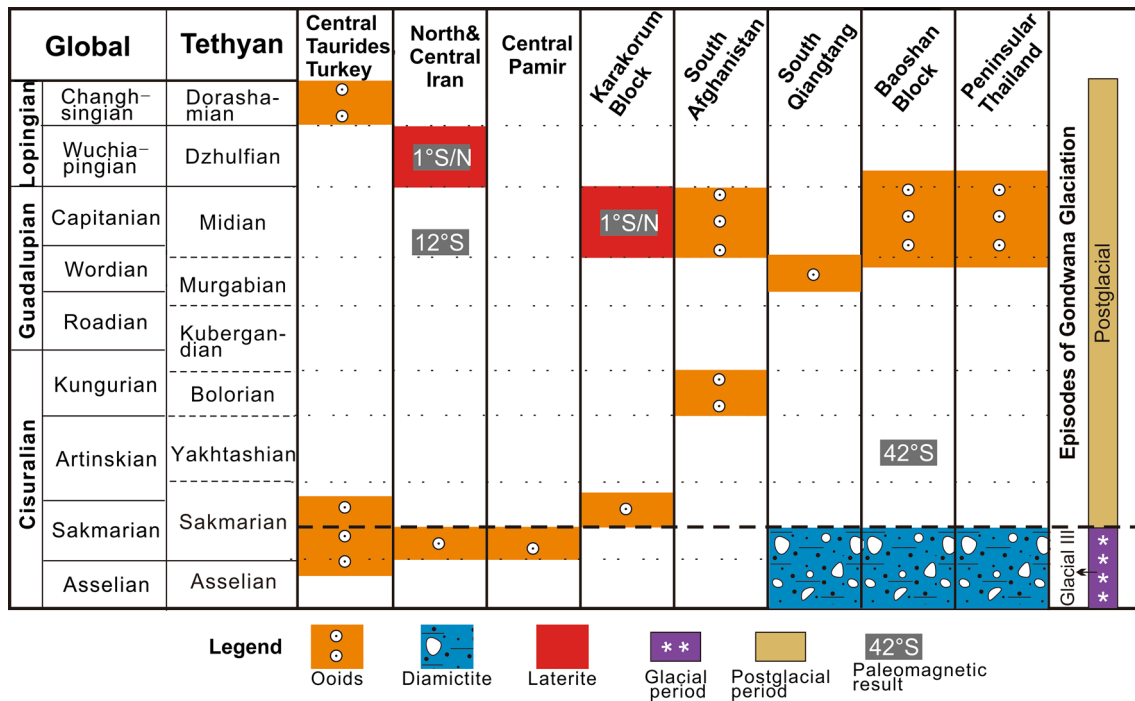
Fig. 9 Comparison of stratigraphic distribution of Permian oolitic carbonates among several Gondwana-derived blocks. Timing of glaciation is based on Isbell et al. (2003, 2012)

of Paleozoic, based on the nature of their crystalline basement and covering Paleozoic successions, as well as paleomagnetic studies (Stöcklin 1974; Berberian and King 1981; Wendt et al. 2005; Angiolini et al. 2007; Muttoni et al. 2009a, b).

To the east of Iran, Permian ooid can be found in South Afghanistan, Central Pamir and Karakorum Block. These three tectonic terranes are evidenced to be of Gondwana provenance by their Paleozoic tectonic evolution and lithologic and faunal successions, especially the Asselian–early Sakmarian bryozoans, bivalves and brachiopods and Sakmarian Kalaktash fusulinid assemblage which indicate cool/temperate-water peri-Gondwana environment (Gaetani et al. 1995; Gaetani 1997; Leven 1997; Angiolini et al. 2005, 2013). In South Afghanistan, Permian oolitic limestones are interbedded with algal-foraminiferal limestones in Bed 7 of the Permian sequence in the Khaftkala zone and attested by advanced *Neoschwagerina* and smaller foraminifera to be Midian in age (Leven 1997, Fig. 10); oolitic beds dated by fusulinids to be Bolorian occur in Zone P3 in the Permian Tezak sequence in the Argandab trough (Leven 1997, Fig. 16). The Permian successions of Central Pamir resemble those of Halvan mountains in Central Iran and contain ooids at the base of the Permian in the Dangikalon Formation at Kalaktash and West Pshart areas (Leven 1993; Leven and Gorgij 2011b, pl. V, Fig. 2). These oolitic beds are overlain by Sakmarian Kalaktash fusulinid

assemblage and bryozoans, but their lower boundary is poorly age-controlled. We tentatively correlate the oolitic beds in Central Pamir to those from Central Iran, based on the similar Early Permian sequence in these two regions. Additionally, the Permian ooids in the northern sedimentary belt of Karakorum Block were illustrated from Member 2 of the Early Permian Lupghar Formation at various localities between Chapursan and Shimshal areas (Gaetani et al. 1995, Fig. 12 and pl. 7, Fig. 3), e.g., Hunza oolitic bars. Gaetani et al. (1995) pointed out that these ooids were immediately underlain by fusulinids correlative to Sakmarian Kalaktash assemblage and overlain by fossil-barren limestones of which an Artinskian age is possible. Gaetani (written communication 2016) confirmed the presence of these Early Permian ooids in the Karakorum Block, although remarked they are rare in strata.

Moving further eastward, Permian ooids have been recovered from South Qiang tang in Tibet and Peninsular Thailand. Oolitic limestones were reported from the Longge Formation in the Ali (Ngari) area of South Qiangtang, Tibet (Liang et al. 1983). A Murgabian age could be assigned to these oolitic beds based on detailed fusulinid biostratigraphy. In Peninsular Thailand, the carbonates containing foraminiferal *Shanita-Hemigordiopsis* assemblage are commonly oolitic (Dawson et al. 1993, Figs. 4.3, 5.1). This particular assemblage was regarded to be a marker for late Murgabian–early Dzhulfian time
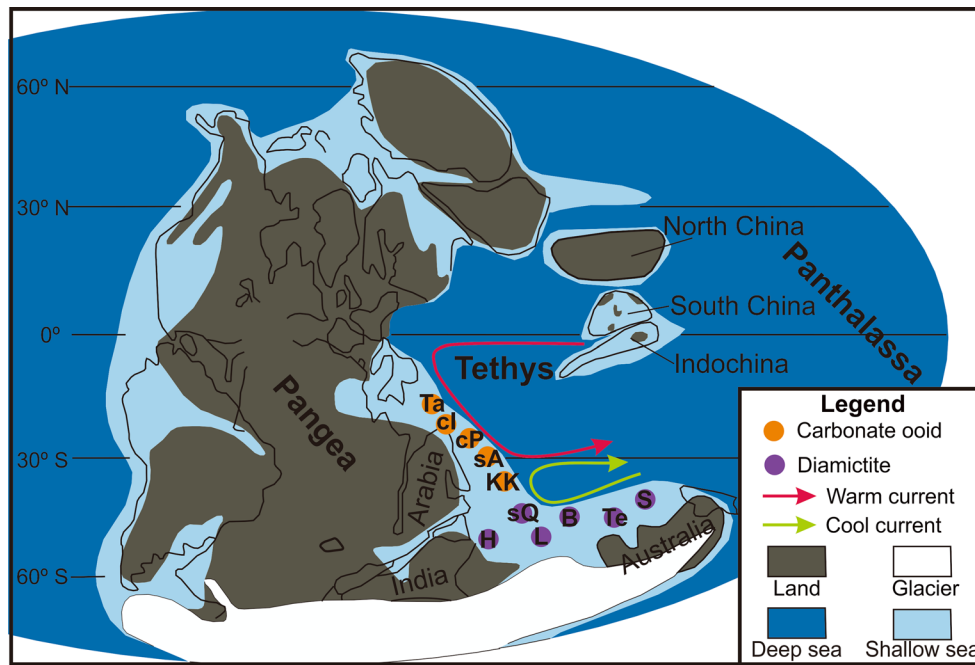
Fig. 10 Schematic paleogeographic map of the Tethyan region during the Early Permian (Asselian–Sakmarian) emphasizing the distribution of carbonate ooids and glaciomarine diamictites among the Gondwana-derived blocks. Modified from the base map from Metcalfe (2013) with additional information from Angiolini et al. (2007), Muttoni et al. (2009a), Ali et al. (2013) and Domeier and Torsvik (2014). Abbreviations for tectonic terranes: Ta—Taurides, Turkey, cI—Central Iran, cP—Central Pamir, sA—South Afghanistan, KK—Karakorum Block, sQ—South Qiangtang, Tibet, B—Baoshan Block, SW China, L—Lhasa Block, Tibet, Te—Tengchong Block, SW China, S—Sibumasu including Peninsular Thailand, H—Himalaya

in Peninsular Thailand (Dawson et al. 1993). Quite similar to the Baoshan Block, the Gondwana ancestry of South Qiangtang and Peninsular Thailand is testified by Early Permian cool/temperate-water fossils of Gondwana affinity and Asselian–Sakmarian glaciomarine diamictites (Ridd 1971; Liang et al. 1983; Jin 2002; Ampaiwan et al. 2009; Metcalfe 2013).

The variable spatio-temporal distribution of Permian ooids among these Gondwana-derived blocks bears paleogeographic significance. Concerning the warm seawater as a prerequisite for ooid production, we interpret the blocks yielding Sakmarian ooids to reside in at least subtropical warm-water realm during the Sakmarian, whereas Baoshan Block as well as South Qiangtang and Peninsular Thailand in cool-water region during the Asselian–Sakmarian time (Fig. 10). Another supporting fact is that no unequivocal Early Permian glaciomarine sediments have hitherto been discovered from these blocks hosting Sakmarian ooids (Sengör et al. 1988; Gaetani et al. 1995; Kobayashi and Altiner 2008; Metcalfe 2013). Such remarkable contrast in sea-surface temperature very likely results from different paleolatitudes of these blocks. During the Permian period, distinct latitudinal temperature gradient and climatic zones have been demonstrated by worldwide data from varying disciplines, such as terrestrial florals and marine invertebrates, computer model simulation and climate-sensitive lithotypes (Dickens 1985; Bambach 1990; Ross 1995, Ziegler et al. 1997, 1998; Rees et al. 1999; Kiessling et al. 1999; Mei and Henderson 2001; Winguth et al. 2002; Angiolini et al. 2007; Boucot et al. 2013). Korte et al. (2008) suggested about 9–12 °C gradient of sea-surface temperature between tropical/subtropical (<30°) and high southern (55 ± 10°) latitude localities, after comparing oxygen isotope values of brachiopod shells from low-latitude and high-latitude habitats. We therefore infer that the Baoshan Block, Peninsular Thailand and South Qiangtang, Tibet, were located at comparatively higher southern latitudes and more severely influenced by the Gondwana glaciation during the Asselian–Sakmarian time than those blocks where Sakmarian ooids were deposited. Another factor affecting sea-surface temperature could be oceanic current circulation. Limited studies have proposed that an equatorial warm current flowed westward and deflected southeastward upon reaching the northern margin of Gondwana, and a clockwise cool current existed at southern mid-latitudes within the Permian Tethys (Kiessling et al. 1999; Yan and Zhao 2001; Winguth et al. 2002; Angiolini et al. 2007). The boundary between the warm and cool currents has been suggested, in these studies, to be roughly around 30°S with warm and cool currents confined, respectively,

in warm and cool climatic belts. This means that the warm current would fail to impact the sea-surface temperature of the cool climatic belt to the south of 30°S, although its northeastward deflection could compensate the decrease of sea-surface temperature toward higher latitudes. Meanwhile, the cool current could not penetrate into the warm climatic belt. Assuming such proposed pattern of ocean gyres is valid, the ocean currents are not supposed to radically modify the overall distinction of sea-surface temperature between warm and cool climatic belts governed by paleolatitudes within the Permian Tethys.

This inferred Asselian–Sakmarian paleoposition of the Baoshan Block agrees well with paleomagnetic and fossil data. Paleomagnetic studies on the basalts of the Woniusi Formation (most likely Artinskian in age) have restored the Baoshan Block to be near the conjunction of northern India and northwestern Australia with a paleolatitude as high as 42°S (Huang and Opdyke 1991; Ali et al. 2013; Xu et al. 2015). For fossils, Cisuralian (Sakmarian to possibly Artinskian) fusulinids of the Baoshan are rather monotonous and represent warm-temperate condition, exclusively comprising *Eoparafusulina* and *Pseudofusulina* (Shi et al. 2011; Huang et al. 2015b). In contrast, Asselian–Sakmarian fusulinids in Central Taurides of Turkey, Central Iran, Central Pamir are not only more diversified but also include subordinate elements of Pseudoschwagerininae (e.g., *Sphaeroschwagerina* and *Chalaroschwgerina*), which are common in tropical/subtropical eastern Tethys (Leven 1993; Kobayashi and Altiner 2008; Leven and Gorgij 2011b).

Quite remarkably, the Middle Permian distribution of carbonate ooids reverses among these Gondwana-derived blocks. During Wordian–Capitanian, ooids made their debut in Baoshan Block, South Qiangtang and Peninsular Thailand, but turned absent in those blocks used to accommodate Sakmarian ooids. Instead, laterites ascribed to warm and humid climate were developed, respectively, in western Karakorum Block during the Capitanian and in North Iran (Alborz Mountains) during the Wuchiapingian (Muttoni et al. 2009a). These laterites have been revealed by paleomagnetic data to be formed near the paleoequator (1°N/S) (Muttoni et al. 2009a). Another estimated paleolatitude of the Alborz region is 12°S for the Wordian–Capitanian time based on paleomagnetic results from lavas interbedded within strata underlying the Alborz laterites (Besse et al. 1998; Muttoni et al. 2009a). In addition, the South China maintained a position nearby paleoequator throughout the Permian (Nie 1991) and was also virtually devoid of carbonate ooids prior to the latest Permian (Yan 2004; Li and Wu 2012; Tian et al. 2014; Li et al 2015b). These observations demonstrate that the ooid distribution in the Permian Tethyan region seems analogous to the present-day situation (Lees 1975; Opdyke and Wilkinson 1990) in that ooids are rather scarce near the equator, notwithstanding

their confinement within tropical/subtropical region. Accordingly, we postulate that the Baoshan Block was situated in the southern mid-latitudes between the paleoequator and 42°S during the Wordian–Capitanian interval. This interpretation is corroborated by faunal features of several fossil taxa. Wang et al. (2001) stated that the Guadalupian coral diversity is much lower in the Baoshan Block than in typical Cathaysian region, e.g., South China. Similarly, Guadalupian fusulinids in the Baoshan Block, especially representatives of Verbeekinidae and Neoschwagerinidae diagnostic for warm water, are much less diversified than their counterparts in South China, as well as Taurides of Turkey, Central Iran and South Afghanistan (Ueno 2003; Huang et al. 2015a, b). Paleobiogeographic studies on Guadalupian brachiopods showed that the affinity of the Baoshan Block was closely related to localities at Gondwana margin and belongs to a southern transitional Cimmerian Province, while the North Karakorum was grouped with South China to a Cathaysian Province in the equatorial belt (Shen et al. 2009; Angiolini et al. 2013). In sum, the Baoshan Block probably lays in tropical/subtropical region at southern mid-latitudes during the Wordian–Capitanian, still remaining to the south of the paleoequator.

Conclusions

Permian oolitic carbonates are confirmed to be extensive in the Baoshan Block in western Yunnan, China, and determined by biostratigraphic analysis to be Wordian–early Wuchiapingian, predominantly Capitanian in age. Four major ooid types are recognized, namely micritic ooids, compound ooids, leached ooids and half-moon ooids. These ooids cogently indicate a warm and shallow-marine environment for the Guadalupian strata of the Baoshan Block. This corroborates previous understanding that the climatic condition significantly ameliorated from the Cisuralian to Guadalupian in the Baoshan Block.

More significantly, diachronous distribution of Permian ooids among the Gondwana-derived blocks provides new constraints, from the sedimentological perspective, on paleogeographic configuration of these blocks. Sakmarian ooids in Central Taurides of Turkey, Central Iran, Central Pamir and Karakorum Block are in sharp contrast with Asselian–Sakmarian glaciomarine diamictites in Baoshan Block, Peninsular Thailand and South Qiangtang. During the Wordian–Capitanian, ooids debuted in Baoshan Block, South Qiangtang and Peninsular Thailand, whereas turned absent in those blocks where Sakmarian ooids used to occur. Such variable ooid occurrences probably reflect latitudinal difference between these blocks in comparison. The Baoshan Block is interpreted to possess significantly higher latitude than those blocks with warm seawater conducive

to ooid formation during the Asselian–Sakmarian and thus more severely influenced by Gondwana glaciation. During the Wordian–Capitanian, the Baoshan Block already drifted to warm-water southern mid-latitudes, but was still to the south of the equatorial belt where North and Central Iran and Karakorum Block already resided during the Capitanian. We believe that oolitic limestones have proved effective for constraining paleogeography of the Gondwana-derived blocks, and they could be a valuable tool in deciphering paleoclimatic and paleogeographic history, especially for far-travelled terranes which experienced dynamic and complex tectonic evolution.

References

Ali JR, Cheung HMC, Aitchison JC, Sun YD (2013) Palaeomagnetic re-investigation of Early Permian rift basalts from the Baoshan Block, SW China: constraints on the site-of-origin of the Gondwana-derived eastern Cimmerian terranes. Geophys J Int 5:650–663

Ampaiwan T, Hisada KI, Charusiri P (2009) Lower Permian glacially influenced deposits in Phuket and adjacent islands, peninsular Thailand. Isl Arc 18:52–68

Angiolini L, Brunton H, Gaetani M (2005) Early Permian (Asselian) brachiopods from Karakorum (Pakistan) and their palaeobiogeographical significance. Palaeontology 48:69–86

Angiolini L, Gaetani M, Muttoni G, Zanchi A (2007) Tethyan oceanic currents and climate gradients 300 m.y. ago. Geology 35:1071–1074

Angiolini L, Zanchi A, Zanchetta S, Nicora A, Vezzoli G (2013) The Cimmerian geopuzzle: new data from South Pamir. Terra Nova 25:352–360

Baccelle L, Bosellini A (1965) Diagrammi per la stima visiva della composizione percentuale nelle rocce sedimentarie. Annali dell'Università di Ferrara (Nuova Serie), Sezione 9, Scienze geologiche e paleontologiche 1:56–62

Bambach RK (1990) Late Palaeozoic provinciality in the marine realm. Mem Geol Soc Lond 12:307–323

Barnaby RJ, Ward WB (2007) Outcrop analog for mixed siliciclastic–carbonate ramp reservoirs—stratigraphic hierarchy, facies architecture, and geologic heterogeneity: Grayburg Formation, Permian basin, U.S.A. J Sediment Res 77:34–58

Bathurst RGC (1966) Boring algae, micrite envelopes and lithification of molluscan biosparites. Geol J 5:15–32

Bathurst RGC (1975) Carbonate sediments and their diagenesis. Elsevier, New York

Berberian M, King GCP (1981) Towards a paleogeography and tectonic evolution of Iran. Can J Earth Sci 18:210–265

Besse J, Torcq F, Gallet Y, Ricou LE, Krystyn L, Saidi A (1998) Late Permian to Late Triassic palaeomagnetic data from Iran: constraints on the migration of the Iranian block through the Tethyan Ocean and initial destruction of Pangea. Geophys J Int 135:77–92

Boucot AJ, Chen X, Scotese CR, Morley RJ (2013) Phanerozoic paleoclimate: an atlas of lithologic indicators of climate, vol 11.

SEPM Concepts in Sedimentology and Paleontology. Society for Sedimentary Geology, Tulsa, Oklahoma, USA

Brönnimann P, Whitttaker JE, Zaninetti L (1978) *Shanita*, a new pillared miliolacean foraminifer from the late Permian of Burma and Thailand. Riv Ital Paleontol Stratigr 84:63–92

Bureau of Geology and Mineral Resources of Yunnan Province (1990) Regional Geology of Yunnan Province. Geological Publishing House, Beijing

Davies PJ, Bubela B, Ferguson J (1978) The formation of ooids. Sedimentology 25:703–729

Dawson O, Racey A, Whittaker JE (1993) The palaeoecological and palaeobiogeographic significance of *Shanita* (Foraminifera) and associated foraminifera/algae from the Permian of Peninsular Thailand. In: Proceedings of international symposium on biostratigraphy of mainland southeast Asia: facies and paleontology, pp 283–298

Deelman JC (1978) Experimental ooids and grapestones: carbonate aggregates and their origin. J Sediment Res 48:503–512

Dickens JM (1985) Late Palaeozoic climate with special reference to invertebrate faunas. In: Dutro JT Jr, Pfefferkorn HW (eds) Compte Rendu Nuevieme Congres International de Stratigraphie et de Geologie du Carbonifere, vol 5. Southern Ilinois University Press, Carbondale, pp 394–402

Domeier M, Torsvik TH (2014) Plate tectonic in the late Paleozoic. Geosci Front 5:303–350

Esteban M, Pray LC (1983) Pisoids and pisolite facies (Permian), Guadalupe Mountains, New Mexico and West Texas. In: Peryt TM (ed) Coated Grains. Springer, Berlin, pp 503–537

Fan JC, Fang RS (1992) Glacier diagenetic features and related problems for Dingjiazhai Formation in Mid-late Carboniferous, Baoshan-Shidian region. Yunnan Geol 11:268–282 **(in Chinese)**

Fang RS (1983) The early Permian brachiopod from Xiaoxinzhai of Gengma, Yunnan and its geological significance. Contrib Geol Qinghai Xizang Tibet Plateau 11:93–112 **(in Chinese)**

Fang RS (1994) The discovery of cold-water brachiopod *Stepanoviella* fauna in Baoshan region and its geological significance. Yunnan Geol 13:264–277 **(in Chinese)**

Fang RS, Fan JC (1994) On the cold water coral *Lytvolasma* fauna in Baoshan-Tengchong region. Yunnan Geol 13:190–201 **(in Chinese)**

Fang ZJ, Wang YJ, Shi GR, Zhou ZC, Xiao YW (2000) On the age of the Dingjiazhai Formation of Baoshan Block, western Yunnan, China—with a discussion on the redeposition hypothesis. Acta Palaeontol Sin 39:267–278 **(in Chinese)**

Ferrari O-M, Hochard C, Stampfli GM (2008) An alternative plate tectonic model for the Palaeozoic–early Mesozoic Palaeotethyan evolution of Southeast Asia (northern Thailand-Burma). Tectonophysics 451:346–365

Flügel E (2010) Microfacies of carbonate rocks. Springer, Berlin

Gaetani M (1997) The Karakorum Block in Central Asia, from Ordovician to Cretaceous. Sediment Geol 109:339–359

Gaetani M, Angiolini L, Garzanti E, Jadoul F, Leven EJ, Nicora A, Sciunnach D (1995) Permian stratigraphy in the northern Karakorum, Pakistan. Riv Ital Paleontol Stratigr 101:107–152

Geological Survey Team of Yunnan (1980) Regional Geological Reports of the Geological Map of Baoshan Sheet (1:200,000). Bureau of Geology and Mineral Resources of Yunnan Province, Kunming

Göncüoğlu MC et al (2007) The Mississippian in the Central And Eastern Taurides (Turkey): constraints on the tectonic setting of the Tauride-Anatolide Platform. Geol Carpath Bratisl 58:427–442

Harris PM (1983) The Joulters ooid shoal, Great Bahama Bank. In: Peryt TM (ed) Coated Grains. Springer, Berlin, pp 132–141

Hearty PJ, Webster JM, Clague DA et al (2010) A pulse of ooid formation in Maui Nui (Hawaiian Islands) during Termination I. Mar Geol 268:152–162

Huang K, Opdyke ND (1991) Paleomagnetic results from the Upper Carboniferous of the Shan-Thai-Malay block of western Yunnan, China. Tectonophysics 192:333–344

Huang H, Yang XN, Jin XC (2005) The *Shantia* fauna (Permian foraminifera) from Baoshan area, western Yunnan. Acta Palaeontol Sin 44:545–555 **(in Chinese)**

Huang H, Jin XC, Shi YK, Yang XN (2009) Middle Permian western Tethyan fusulinids from southern Baoshan Block, western Yunnan, China. J Palaeontol 83:880–896

Huang H, Jin XC, Shi YK (2015a) A *Verbeekina* assemblage (Permian fusulinid) from the Baoshan Block in western Yunnan, China. J Palaeontol 89:269–280

Huang H, Shi YK, Jin XC (2015b) Permian fusulinid biostratigraphy of the Baoshan Block in western Yunnan, China with constraints on paleogeography and paleoclimate. J Asian Earth Sci 104:127–144

Huang H, Shi YK, Jin XC (2016) Permian (Guadalupian) fusulinids of Bawei Section in Baoshan Block, western Yunnan, China: biostratigraphy, facies distribution and paleogeographic discussion. Palaeoworld. doi:10.1016/j.palwor.2016.03.004

Isbell JL, Miller MF, Wolfe KL, Lenaker PA (2003) Timing of late Paleozoic glaciation in Gondwana: Was glaciation responsible for the development of northern hemisphere cyclothems? In: Chan MA, Archer AW (eds) Extreme depositional environments: mega end members in geological times. Geological Society of America, Sepcial Paper 370. Geological Society of America, Boulder, Colorado, pp 5–24

Isbell JL, Henry LC, Gulbranson EL et al (2012) Glacial paradoxes during the late Paleozoic ice age: evaluating the equilibrium line altitude as a control on glaciation. Gondwana Res 22:1–19

James NP (1997) The cool-water depositional realm. In: James NP, Clarke NP (eds) Cool-water carbonates. Society of Economic Paleontologists and Mineralogists, Special Publication 56, Tulsa Oklahoma, USA, pp 1–20

Jin XC (1994) Sedimentary and paleogeographic significance of Permo-Carboniferous sequences in western Yunnan, China. PhD Dissertation, University of Koeln

Jin XC (2002) Permo-Carboniferous sequences of Gondwana affinity in Southwest China and their paleogeographic implications. J Asian Earth Sci 20:633–646

Jin XC, Yang XN (2004) Paleogeographic implications of the *Shanita-Hemigordius* fauna (Permian foraminifer) in the reconstruction of Permian Tethys. Episodes 27:273–278

Jin XC, Zhan LP (2008) Spatial and temporal distribution of the *Cryptospirifer* fauna (Middle Permian brachiopods) in the Tethyan realm and its paleogeographic implications. Acta Geol Sin 82:1–16

Jin Y, Bruce RW, Brian FG, Galina VK (1997) Permian chronostratigraphic subdivisions. Episodes 20:10–15

Jin XC, Huang H, Shen Y, Wang YZ (2008) Subdivision and correlation of Mid-Late Permian successions of the Baoshan Block, western Yunnan: status and Problems. Acta Geos Sin 29:533–541 **(in Chinese)**

Jin XC, Huang H, Shi YK, Zhan LP (2011) Lithologic boundaries in Permian post-glacial sediments of the Gondwana-affinity regions of China: typical sections, age range and correlation. Acta Geol Sin 85:373–386

Kiessling W, Flügel E, Golonka J (1999) Paleoreef maps: evaluation of a comprehensive database on Phanerozoic reefs. AAPG Bull 83:1552–1587

Kobayashi F, Altiner D (2008) Fusulinoidean faunas from the Upper Carboniferous and Lower Permian platform limestone in the Hadim area, Central Taurides, Turkey. Riv Ital Paleontol Stratigr 114:191–232

Korte C, Jones PJ, Brand U, Mertmann D, Veizer J (2008) Oxygen isotope values from high-latitudes: Clues for Permian

sea-surface temperature gradients and Late Palaeozoic deglaciation. Palaeogeogr Palaeoclimatol Palaeoecol 269:1–16

Lan CH, Sun C, Fan JC, Fang RS (1983) Carboniferous and Permian stratigraphy of the Zhenkang and Luxi region in western Yunnan. Contrib Geol Qinghai Xizang Tibet Plateau 11:79–92 **(in Chinese)**

Lees A (1975) Possible influence of salinity and temperature on modern shelf carbonate sedimentation. Mar Geol 19:159–198

Lees A, Buller AT (1972) Modern temperate-water and warm-water shelf carbonate sediments contrasted. Mar Geol 13:67–73

Leven EJ (1993) Early Permian fusulinids from the central Pamir. Riv Ital Paleontol Stratigr 99:151–198

Leven EJ (1997) Permian stratigraphy and fusulinida of Afghanistan with their paleogeographic and paleotectonic implications. Geol Soc Am Spec Pap 316:1–134

Leven EJ, Gorgij MH (2011a) Fusulinids and stratigraphy of the Carboniferous and Permian in Iran. Stratigr Geol Correl 19:687–776

Leven EY, Gorgij MN (2011b) The Kalaktash and Halvan assemblages of Permian fusulinids in the Padeh and Sang-Variz sections (Halvan Mountains, Yazd Province, central Iran). Stratigr Geol Correl 19:20–39

Li F, Wu X (2012) Characteristics and palaeoenvironmental significances of shallow-marine sediments in the latest Permian, Moyang Section, Guizhou. Acta Sedimentol Sin 30:679–688 **(in Chinese)**

Li F, Wu SQ, Liu K (2015a) Identification of ooid primary mineralogy: a clue for understanding the variation in paleo-oceanic chemistry. Acta Sedimentol Sin 33:500–511 **(in Chinese)**

Li F, Yan JX, Chen ZQ, Ogg JG et al (2015b) Global oolite deposits across the Permian-Triassic boundary: a synthesis and implications for palaeoceanography immediately after the end-Permian biocrisis. Earth Sci Rev 149:163–180

Liang D, Nie Z, Guo T, Xu B, Zhang Y, Wang W (1983) Permo-Carboniferous Gondwana-Tethys facies in southern Karakorum Ali, Xizang (Tibet). Earth Sci J Wuhan College Geol 19:9–27

Liu BJ, Feng QL, Chonglakmani C, Helmcke D (2002) Framework of paleotethyan archipelago ocean of western Yunnan and its elongation towards north and south. Earth Sci Front 9:161–171 **(in Chinese)**

Mei S, Henderson CM (2001) Evolution of Permian conodont provincialism and its significance in global correlation and paleoclimate implication. Palaeogeogr Palaeoclimatol Palaeoecol 170:237–260

Metcalfe I (2013) Gondwana dispersion and Asian accretion: Tectonic and palaeogeographic evolution of eastern Tethys. J Asian Earth Sci 66:1–33

Moix P, Beccaletto L, Kozur HW, Hochard C, Rosselet F, Stampfli GM (2008) A new classification of the Turkish terranes and sutures and its implication for the paleotectonic history of the region. Tectonophysics 451:7–39

Muttoni G, Kent DV, Garzanti E et al (2009a) Opening of the Neo-Tethys Ocean and the Pangea B to Pangea A transformation during the Permian. Geoarabia 14:17–48

Muttoni G, Mattei M, Balini M et al (2009b) The drift history of Iran from the Ordovician to the Triassic. Geol Soc Lond Spec Publ 312:7–29

Nelson CS (1988) An introductory perspective on non-tropical shelf carbonates. Sediment Geol 60:3–12

Newell ND, Purdy EG, Imbrie J (1960) Bahamian oolitic sand. J Geol 68:481–497

Nie S (1991) Paleoclimatic and paleomagnetic constraints on the Paleozoic reconstruction of south China, north China and Tarim. Tectonophysics 196:279–308

Okuyucu C (2008) Biostratigraphy and systematics of late Asselian-early Sakmarian (Early Permian) fusulinids (foraminifera) from southern Turkey. Geol Mag 145:413–434

Opdyke BN, Wilkinson BH (1990) Paleolatitude distribution of Phanerozoic marine ooids and cements. Palaeogeogr Palaeoclimatol Palaeoecol 78:135–148

Peryt TM (1983) Coated Grains. Springer, Berlin

Pierre A, Durlet C, Razin P, Chellai EH (2010) Spatial and temporal distribution of ooids along a Jurassic carbonate ramp: Amellago transect, High-Atlas, Morocco. Geol Soc Lond Spec Publ 329:65–88

Pronina GP (1988) The Late Permian smaller foraminifera of Transcaucasus. Revue de Paleobiologie Vol Spec 2:89–96

Rankey EC, Reeder SL (2009) Holocene ooids of Aitutaki Atoll, Cook Islands, South Pacific. Geology 37:971–974

Rankey EC, Reeder SL (2011) Holocene oolitic marine sand complexes of the Bahamas. J Sediment Res 81:97–117

Reeder SL, Rankey EC (2008) Relations between sediments and tidal flows in ooid shoals, Bahamas. J Sediment Res 78:175–186

Rees PM, Gibbs MT, Ziegler AM, Kutzbach JE, Behling PJ (1999) Permian climates: Evaluating model predictions using global paleobotanical data. Geology 1(27):891–894

Reid RP, Macintyre IG (2000) Microboring versus recrystallization: further insight into the micritization process. J Sediment Res 70:24–28

Richter DK (1983) Calcareous ooids: a synopsis. In: Peryt TM (ed) Coated grains. Springer, Berlin, pp 71–99

Ridd MF (1971) South-East Asia as a Part of Gondwanaland. Nature 234:531–533

Ross CA (1995) Permian fusulinaceans. In: Scholle PA, Peryt TM, Ulmer-Scholle DS (eds) The Permian of Northern Pangea. Springer, Berlin, pp 167–185

Sandberg PA (1983) An oscillating trend in Phanerozoic non-skeletal carbonate mineralogy. Nature 305:19–22

Scotese CR (2004) A continental drift flipbook. J Geol 112:729–741

Sengör AM (1979) Mid-Mesozoic closure of Permo-Triassic Tethys and its implications. Nature 279:590–593

Sengör AM, Altiner D, Cin A, Ustaomer PA, Hsu KJ (1988) Origin and assembly of the Tethyside orogenic collage at the expense of Gondwanaland. In: Audley-Charles MG, Hallam A (eds) Geological Society Special Publications, vol 37, pp 81–119

Shahraki J, Javdan MJ, Hashemi SMP, Jami M, Nastooh M, Kalvandi SM (2015) Facies Analysis, Depositional Environment of the Lower Permian Deposits of Chili Formation in Kalmard Block, Eastern Central Iran (Darin Section). Open J Geol 5:539–551

Sheng JZ, He Y (1983) Permian *Shanita-Hemigordius* (*Hemigordiopsis*) (foraminifera) fauna in western Yunnan, China. Acta Palaeontol Sin 22:55–60

Shen SZ, Xie JF, Zhang H, Shi GR (2009) Roadian-Wordian (Guadalupian, Middle Permian) global palaeobiogeography of brachiopods. Glob Planet Chang 65:166-181. doi:10.1016/j.gloplacha.2008.10.017

Shi GR, Archbold NW (1998) Permian marine biogeography of SE Asia. In: Hall R, Holloway JD (eds) Biogeography and Geological Evolutions of SE Asia. Backhuys Publishers, Leiden, pp 57–72

Shi GR, Shen SZ (2001) A biogeographically mixed Middle Permian brachiopod fauna from the Baoshan Block, western Yunnan, China. Palaeontology 44:237–258

Shi GR, Fang ZJ, Archbold NW (1996) An Early Permian brachiopod fauna of Gondwanan affinity from the Baoshan block, western Yunnan, China. Alcheringa 20:81–101

Shi YK, Huang H, Jin XC, Yang XN (2011) Early Permian fusulinids from the Baoshan Block, western Yunnan, China and their paleobiogeographic significance. J Palaeontol 85:489–501

Simone L (1980) Ooids: a review. Earth Sci Rev 16:319–355

Stöcklin J (1974) Possible ancient continental margins in Iran. In: Burk CA, Drake CL (eds) The geology of continental margins. Springer, Berlin, pp 873–887

Strasser A (1986) Ooids in Purbeck limestones (lowermost Cretaceous) of the Swiss and French Jura. Sedimentology 33:711–727

Tewari VC, Tucker ME (2011) Ediacaran Krol carbonates of the Lesser Himalaya, India: Stromatolitic facies, depositional environment and diagenesis. In: Tewari VC, Seckbach J (eds) Stromatolites: interaction of microbes with sediments, vol 18., Cellular origin, life in extreme habitats and astrobiologySpringer, Dordrecht, pp 133–156

Tian L, Tong JN, Sun DL et al (2014) The microfacies and sedimentary responses to the mass extinction during the Permian-Triassic transition at Yangou Section, Jiangxi Province, South China. Sci China Earth Sci 57:1–13

Tucker ME, Wright VP, Dickson JAD (1990) Carbonate Sedimentology. Blackwell Science, Oxford

Ueno K (2003) The Permian fusulinoidean faunas of the Sibumasu and Baoshan blocks: their implications for the paleogeographic and paleoclimatologic reconstruction of the Cimmerian Continent. Palaeogeogr Palaeoclimatol Palaeoecol 193:1–24

Ueno K, Mizuno Y, Wang XD, Mei SL (2002) Artinskian conodonts from the Dingjiazhai formation of the Baoshan Block, west Yunnan, southwest China. J Palaeontol 76:741–750

Ünal E, Altiner D, Ömer Yilmaz I, Özkan-Altiner S (2003) Cyclic sedimentation across the Permian-Triassic boundary (Central Taurides, Turkey). Riv Ital Paleontol Stratigr 109:359–376

Wang YZ (1983) The characteristics and significance of Carboniferous gravel bed in Tengchong and Baoshan area, western Yunnan. Contrib Geol Qinghai Xizang Tibet Plateau 11:71–75 **(in Chinese)**

Wang XD, Ueno K, Mizuno Y, Sugiyama T (2001) Late Paleozoic faunal, climatic, and geographic changes in the Baoshan block as a Gondwana-derived continental fragment in Southwest China. Palaeogeogr Palaeoclimatol Palaeoecol 170:197–218

Wendt J, Kaufmann B, Beilka Z, Farsan N, Bavandpur AK (2005) Devonian/Lower Carboniferous stratigraphy, facies patterns and palaeogeography of Iran Part II. Northern and central Iran. Acta Geol Pol 55:31–97

Wilkinson BH, Buczynski C, Owen RM (1984) Chemical control of carbonate phases: implications from Upper Pennsylvanian calcite-aragonite ooids of southeastern Kansas. J Sediment Res 54:932–947

Win Z, Aung HH, Shwe KK (2011) *Shanita thawtini*, a new milioloid foraminifer from the Middle Permian of Myanmar. Micropaleontology 57:125–137

Winguth AME et al (2002) Simulated warm polar currents during the middle Permian. Paleoceanography 17:9-1–9-18

Wopfner H (1996) Gondwana origin of the Baoshan and Tengchong terranes of West Yunnan. In: Hall R, Blundell D (eds) Tectonic Evolutions of Southeast Asia, Geological Society London, Special Publication 106, pp 539–547

Wopfner H, Jin XC (2009) Pangea megasequences of Tethyan Gondwana-margin reflect global changes of climate and tectonism in Late Palaeozoic and Early Triassic times—a review. Palaeoworld 18:169–192

Xu Y, Yang Z, Tong YB, Wang H, Gao L, An C (2015) Further paleomagnetic results for lower Permian basalts of the Baoshan Terrane, southwestern China, and paleogeographic implications. J Asian Earth Sci 104:99–114

Yan JX (2004) Origin of Permian Chihsian carbonates from South China and its geological implications. Acta Sedimentol Sin 22:579–587 **(in Chinese)**

Yan JX, Liang DY (2005) Early and Middle Permian paleoclimates of the Baoshan Block, western Yunnan, China: insight from carbonates. J Asian Earth Sci 24:753–764

Yan JX, Zhao K (2001) Permo-Triassic paleogeographic, paleoclimatic and paleoceanographic evolutions in eastern Tethys and their coupling. Sci China Ser D 44:968–978

Yang XN, Jin XC, Ji ZS et al (2004) New materials of the *Shanita-Hemigordius* assemblage (Permian foraminifers) from the Baoshan Block, western Yunnan. Acta Geol Sin 78:15–21

Zeng YF, Lee NH, Huang YZ (1983) Sedimentary characteristics of oolitic carbonates from the Jialing-Jiang Formation [Lower Triassic T2 1J1], South Sichuan Basin, China. In: Peryt TM (ed) Coated grains. Springer, Berlin, pp 176–187

Ziegler AM, Hulver ML, Rowley DB (1997) Permian world topography and climate. In: Martini IP (ed) Late glacial and postglacial environmental changes; Quaternary, Carboniferous-Permian, and Proterozoic. Oxford University Press, New York, pp 111–142

Ziegler AM, Gibbs MT, Hulver ML (1998) A mini-atlas of oceanic water masses in the Permian period. In: Shi GR, Archbold NW, Grover M (eds) Strzelecki Symposium on the Permian of Eastern Tethys: Biostratigraphy, Palaeogeography and Resources. The Royal Society of Victoria, Victoria, pp 323–344